



Engineering a thermo-stable superoxide dismutase functional at sub-zero to $>50^{\circ}\text{C}$, which also tolerates autoclaving

Arun Kumar, Som Dutt, Ganesh Bagler, Paramvir Singh Ahuja & Sanjay Kumar

Biotechnology Division, CSIR-Institute of Himalayan Bioresource Technology (Council of Scientific and Industrial Research, India), Palampur-176 061, Himachal Pradesh, India.

SUBJECT AREAS:

PLANT CELL BIOLOGY

GENES

BIOINFORMATICS

COMPUTATIONAL BIOLOGY

Received

13 February 2012

Accepted

27 March 2012

Published

30 April 2012

Correspondence and requests for materials should be addressed to S.K. (sanjaykumar@ihbt.res.in; sanjayplp@rediffmail.com)

Superoxide dismutase (SOD) is a critical enzyme associated with controlling oxygen toxicity arising out of oxidative stress in any living system. A hyper-thermostable SOD isolated from a polyextremophile higher plant *Potentilla atrosanguinea* Lodd. var. *argyrophylla* (Wall. ex Lehm.) was engineered by mutation of a single amino acid that enhanced the thermostability of the enzyme to twofold. The engineered enzyme was functional from sub-zero temperature to $>50^{\circ}\text{C}$, tolerated autoclaving (heating at 121°C , at a pressure of 1.1 kg per square cm for 20 min) and was resistant to proteolysis. The present work is the first example to enhance the thermostability of a hyper-thermostable protein and has potential to application to other proteins for enhancing thermostability.

Copper, zinc superoxide dismutase (Cu,Zn SOD; EC 1.15.1.1) catalyzes a two-step dismutation of the toxic superoxide radical (O_2^-) to molecular oxygen and hydrogen peroxide through alternate reduction and oxidation of copper ion at diffusion-limited catalytic rate¹⁻³. Cu,Zn SOD forms the first line of defense in all aerobic organisms against reactive oxygen radicals and is vital to the survival of cells⁴. Therefore, SOD is an important enzyme for aerobic organisms including plants and humans and also in those applications which require scavenging of O_2^- ⁵⁻⁷.

Eukaryotic Cu,Zn SODs display conserved three dimensional fold built on a flattened Greek key motif and are homodimeric with two subunits held together by hydrophobic interactions^{8,9}. Several reports suggested dimeric structure of Cu,Zn SOD to be more stable with superior activity¹⁰⁻¹², though in *Escherichia coli* this did not appear to be the case¹³. Cu,Zn SODs are known stable enzymes since these tolerate 8 M urea¹⁴ and 4% sodium dodecyl sulfate¹⁵. Various factors responsible for imparting stability/thermo-stability include relatively small solvent-exposed surface area, increased packing density that reduces cavities in the hydrophobic core, an increase in core hydrophobicity, hydrogen bonds between polar residues, increased occurrence of proline residues in loops, decreased occurrence of thermolabile residues, increased helical content, increased polar surface area, extensive ion-pair networks and better salt bridge formation^{8,16,17}.

A unique Cu,Zn SOD (WT) in *P. atrosanguinea* was identified by our group⁵ that was functional at sub-zero temperature to $>50^{\circ}\text{C}$ and also the protein retained activity after autoclaving (heating at 121°C , at a pressure of 1.1 kg per square cm for 20 min). The enzyme was identified as a dimer consisting of two asymmetric subunits A and B⁸. Each subunit of the enzyme consisted of eight stranded β - sandwich (1a-8h) connected by seven loops (I-VII), one short helix and one 3_{10} helix. Since increased thermostability is an important desirable feature for Cu,Zn SOD⁶, there is a need to develop methods to improve thermostability of the enzyme.

Several studies showed the importance of single amino acid substitution in modulating kinetic properties of enzymes^{11,18-20}. We developed seven mutants by replacing amino acids at targeted positions by site-directed mutagenesis wherein both subunits of the enzyme had desired mutations. For example, amino acids in the electrostatic loop are important as these determine the shape and strength of the electrostatic field around the active site⁸. Accordingly, two important charged residues in the electrostatic loop, Leu-132 and Ser-135 were replaced by Glu and Lys in two separate mutations. Alanine at position 4 is yet an important amino acid, wherein mutation is reported to cause amyotrophic lateral sclerosis in human²¹. In WT, glycine is present at position 4 and this was mutated to Ala and Ile in two separate mutations. All of these mutations decreased the specific activity of the enzyme and also the tolerance to autoclavability got reduced (Supplementary Fig. S1).



Presence of cysteine in SOD has drawn considerable attention. Mutation of cysteines involved in disulphide linkage results in destabilization of Cu,Zn SOD²². However, mutation of free cysteine increased greater resistance to thermal inactivation¹⁸. Experimental evidence for the enhanced thermo-stability of the Cys (free) → Ala substitution of enzymes has been reported for Cu,Zn SOD from *Bos taurus*¹⁸, *Danio rario*¹⁹, *Xenopus laevis*²⁰, and an esterase from *Bacillus stearothermophilus*²³. Cu,Zn SODs from yeast and *E. coli*, which have no free cysteine residues, show partial and full reversibility after heating at temperatures above their melting temperatures^{24,25}. However, Cu,Zn SOD from *Photobacterium leiognathi* is denatured irreversibly despite having no free cysteine residues²⁶. These results suggested that the free cysteine might or might not be related to the thermal stability of Cu,Zn SOD. Further, studies for characterization of thermo-stability of Cu,Zn SODs had been carried out with emphasis on thermodynamic parameters and the absence of data on enzyme activity posed a question on functionality of the enzyme.

WT enzyme had three cysteine residues at positions 56, 95 and 145, out of which Cys-56 and Cys-145 participated in the formation of disulfide linkage, whereas Cys-95 remained free⁸. The role of free cysteine in regulating the kinetic properties varies, possibly depending upon structure of the protein and hence the amino acid sequence of the protein. So far structural information of Cu,Zn SODs from three plant species namely *P. atrosanguinea* (PDB ID: 2Q2L), *Spinacea oleracea* (PDB ID: 1SRD), and *Solanum lycopersicum* (PDB IDs: 3 MKG, 3 KM1, 3 KM2, 3 HOG) is known. However, the study of molecular determinants for structural-functional aspects of plant SODs is not yet reported.

The objective of the present work was to study the role of cysteine in governing the kinetic properties of Cu,Zn SOD of *P. atrosanguinea* with the background that there is no such knowledge existing for plant Cu,Zn SODs, and that plant and the animal Cu,Zn SODs are structurally very different to each other⁷. Since SODs have enormous implications to the living world due to their role in scavenging superoxide radicals, the present work provides a highly flexible yet stable Cu,Zn SOD at varying temperature.

Results

Native SOD enzyme is being referred to as wild-type (WT), whereas mutant SODs in which Cys-56, Cys-95, Cys-145 were replaced with Ala will be referred to as C56A, C95A, and C145A, respectively in the present work.

The free cysteine on the interface potentially mediates key dimer interactions. To understand the possible role of free Cys-95, the interface residues and their interactions were studied *in silico*. Using relative difference in solvent accessibility criterion of POLYVIEW server²⁷, residues on the dimer interface were identified. Eight residues on chain A (Thr-17, Leu-19, Thr-31, Asn-33, Asp-91, Thr-93, Cys-95, Phe-97) and 6 residues (Glu-12, Asn-54, Met-57, Leu-132, Gly-140, Gly-141) on chain B were predicted to be on the dimer interface (Supplementary Fig. S2). It was observed that the dimer interface has 8 hydrophilic residues (out of 14 predicted to be on the interface) including free Cys-95. Graph-theoretical analysis indicated that Cys-95 residue on the interface is in close structural proximity of other interface residues via short- and long-range contacts. Cys-95 was in direct long-range contact with two other residues on the interface: Thr-31 and Asn-33. Cys-95 interacted via back-bone contacts with Thr-93, and through non-covalent interaction with Phe-97 (one-residue-apart) and Asn-91 (three-residue-apart). These contact network based observations, relying on structurally critical long-range contacts, proposed a role of Cys-95 in oligomerization of WT through interface forming and stabilizing contacts of WT dimer (Supplementary Fig. S3).

The cysteines involved in native disulphide bond formation are part of ‘Critical Interaction Residue Clique (CIRC)’. A CIRC was identified by graph-theoretical modeling of the WT native-state structure. The long-range interaction network (LIN) model suggested a CIRC comprising of four residues that formed a strong long-range clique. Residues Cys-56, Val-117, Ala-144, and Cys-145 were predicted to be critical for the structural stability (Supplementary Fig. S4). Thus, graph-theoretical modeling located the cluster of residues that holds different secondary structures together, apart from identifying the native disulphide forming cysteines (Cys-56 and Cys-145) as a part of CIRC.

Mutation of free cysteine enhances monomer-dimer ratio. WT and C95A existed in monomeric and dimeric form when electrophoresed on 15% SDS-PAGE under non-reducing conditions [without 2-mercaptoethanol (2-ME)]. Whereas, C56A and C145A exhibited multiple bands due to possible oligomerization/aggregation. A noticeable result was a substantial increase in monomer to dimer ratio for C95A as compared to the WT (Fig. 1a). Monomer and dimer of WT and C95A exhibited SOD activity on SDS-PAGE, whereas no SOD activity was detected on the lanes loaded with C56A and C145A (Supplementary Fig. S5). Isolation of monomer and dimer by size exclusion chromatography (Fig. 1b) followed by protein quantification showed that monomer to dimer ratio for the WT and C95A was 1.3 ± 0.2 and 42.8 ± 1.0 , respectively (Fig. 1b). Monomer and dimer of the corresponding peaks were also confirmed by SDS-PAGE analysis under reducing and non-reducing conditions (Fig. 1c), and the identified peaks exhibited SOD activity (Fig. 1b). Since C56A and C145A did not exhibit SOD activity, monomers, dimer and oligomers were not purified for these two cases. It was observed that the monomeric form of SOD migrated as a closely spaced doublet on SDS-PAGE. The closely spaced protein bands in doublets were confirmed to be identical as evidenced by N-terminal amino acid sequencing (described in Supplementary Methods) that exhibited identical amino acid sequences MRGSHHHHHHGS. Data was further supported by mass analysis using a MALDI-TOF (AXIMA-CFR Plus spectrometer, Shimadzu-Kratos, UK) that yielded a mass of 17.39 kDa for WT (Supplementary Fig. S6). The value was in agreement with those obtained by SDS-PAGE (Supplementary Fig. S7) and *in silico* analysis (www.expasy.org) that deduced a mass of 17.4 kDa for the WT. WT/C56A/C95A/C145A is induced in a relatively higher quantity as compared to the individual native proteins in *E. coli* (Supplementary Fig. S7) and it appears that a part of the induced protein acquired a differential tertiary structure leading to differential levels of SDS-loading and hence different migration of polypeptide-SDS complex on SDS-PAGE²⁸.

Cysteine replacement affects SOD activity at different temperatures without affecting pH optima. Enzymatic activity of SOD was checked on a non-denaturing PAGE by activity staining followed by spectrophotometric-based assay. SOD activity for WT and C95A was detectable as opposed to C56A and C145A, which did not exhibit any activity (Fig. 2a). Spectrophotometric-based data showed a higher specific activity of C95A as compared to WT by $5.0 \pm 0.6\%$. After autoclaving, WT lost $17 \pm 4\%$ of the un-autoclaved activity, whereas this loss in activity for C95A was only $8 \pm 2\%$ (Fig. 2a). Since no SOD activity was detectable for C56A and C145A, these were not evaluated for other enzymatic studies. WT exhibited maximum activity at 0–4°C whereas it was at 10°C for C95A (Fig. 2b). WT and C95A were active at zero and sub-zero temperatures. Autoclaved WT exhibited 50% of maximum activity of un-autoclaved enzyme between 30–40°C, whereas it was observed between 50–65°C for C95A.

Interestingly, assay of WT and C95A at pH ranging between 6 to 9 showed that the mutation of Cys-95 did not affect the pH optima of 7.8 (Supplementary Fig. S8).

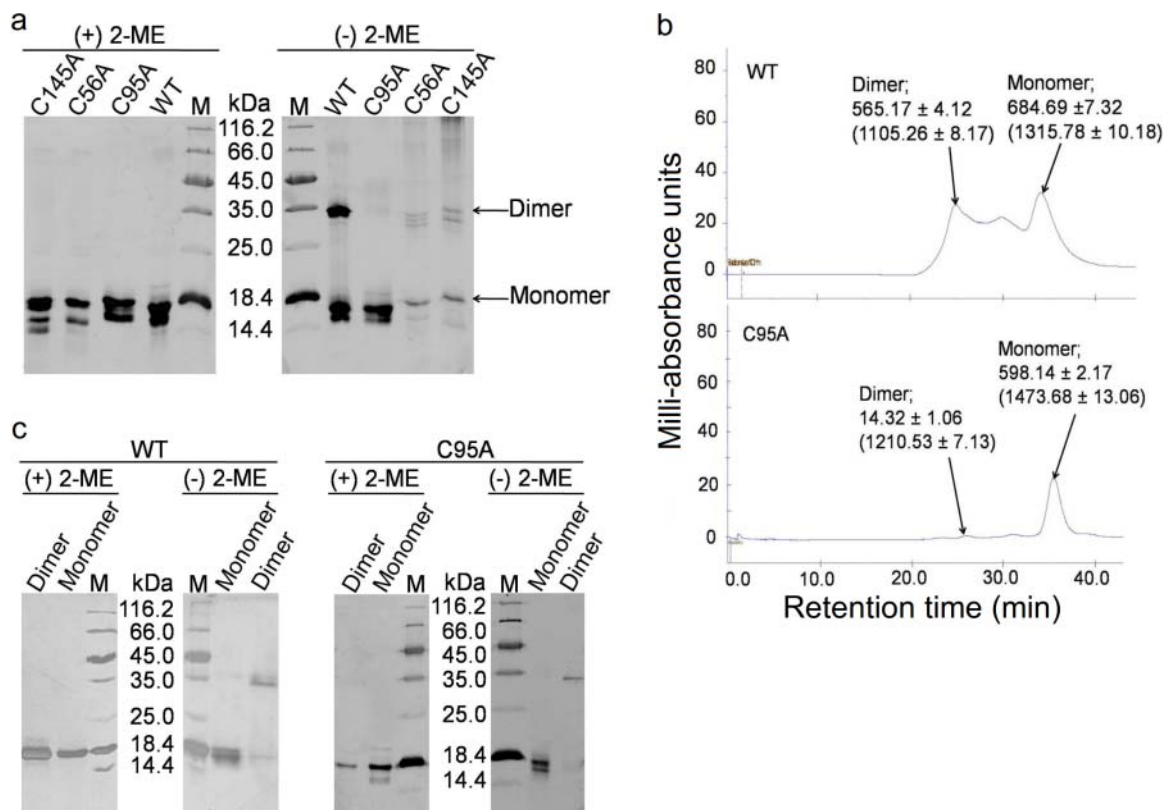


Figure 1 | Analyses of aggregation pattern (including monomer to dimer) of WT and mutant enzymes. One μg of each WT and mutant proteins was loaded separately onto 15% SDS-PAGE in the presence (+) and absence (-) of 2-ME in the sample loading buffer⁵⁰ (a). The name of sample is given above top of each panel. M, molecular weight marker procured from Fermentas, USA; the protein markers were- β -galactosidase (11 6000 Da), bovine serum albumin (66 200 Da), Ovalbumin, 45 000 Da), lactate dehydrogenase (35 000 Da), REase Bsp981 (21 000), β -lactoglobulin (18 400) and lysozyme (14 400 Da)]. SODs analyzed as in (a) were also stained for SOD activity (Supplementary Fig. S5) wherein the said activity was detected for WT and C95A, but not for C56A and C145A. Monomer and dimer observed in panel “a” were separated by size exclusion chromatography (b) for which the purified protein after Ni-NTA chromatography was used as described in Methods section. Numerical values below monomer and dimer represent the amount of protein (μg) as measured by Bradford’s reagent⁴⁸ (Sigma, USA), whereas those in parentheses are the specific activity of SOD (units/mg protein). Separated monomer and dimer of the corresponding peaks in panel “b” were also checked on a 15% SDS-PAGE in the presence (+) and absence (-) of 2-ME included in the sample loading buffer (c). Due to large variation in the protein content in the peaks, equal quantity of protein could not be used for the loading. M, molecular weight marker as in “a”; WT, wild type; C56A, cysteine at position 56 substituted with alanine; C95A, cysteine at position 95 substituted with alanine; C145A, cysteine at position 145 substituted with alanine.

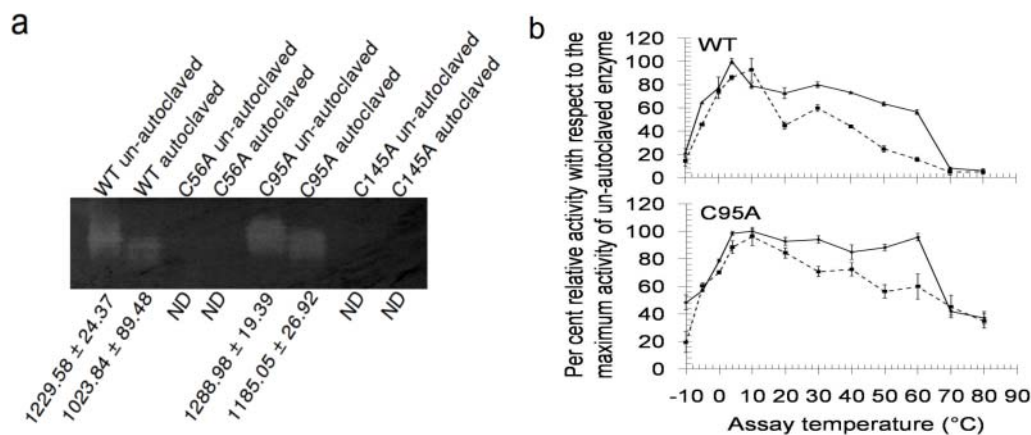


Figure 2 | Effect of cysteine replacement on the activity of SOD. Activity staining gel showing the effect of Cys→Ala replacement on SOD activity (a). Equal quantity (300 ng) of each un-autoclaved and auto-claved WT and mutants was loaded onto 10% native-PAGE and stained for activity^{46,47}. Names of the protein samples are shown at the top of each panel whereas specific activities are given at the bottom of the panel. Enzyme activity was expressed as unit/mg of protein. Values were mean \pm SE of three separate replicates. ND, not detectable. Effect of assay temperature on SOD activity is given in panel (b). Per cent relative activity with respect to the maximum activity across the temperature range is shown. Solid and dashed lines represent un-autoclaved and auto-claved enzymes, respectively. Values were mean \pm SE of three separate replicates. WT, wild type; C56A, cysteine at position 56 substituted with alanine; C95A, cysteine at position 95 substituted with alanine; C145A, cysteine at position 145 substituted with alanine.



Mutation of free cysteine improves resistance to thermal inactivation. Residual SOD activity of WT was $48.0 \pm 1.4\%$, as compared to $69.0 \pm 3.4\%$ for C95A after heating for 160 min at 80°C . Thermal inactivation data exhibited the most linear relationship when plotted at first-order kinetics (Fig. 3) which yielded correlation coefficient (r) of -0.97 and -0.98 for WT and C95A, respectively. Thermal inactivation rate constant (k_d) decreased from a value of $4.6 \pm 0.2 \times 10^{-3} \text{ min}^{-1}$ for WT to $2.4 \pm 0.3 \times 10^{-3} \text{ min}^{-1}$ for C95A. Concomitantly, the half-time of thermal inactivation ($t_{1/2}$) at 80°C increased from 151 ± 6 min for WT to 345 ± 36 min for C95A (Fig. 3 and Supplementary Table S1). The kinetic data showed improved resistance of C95A towards thermal inactivation, as compared to the WT.

WT and C95A tolerate limited proteolysis. WT and C95A exhibited proteolytic tolerance. The digestion patterns as detected by SDS-PAGE revealed partial hydrolysis of WT and C95A with trypsin, chymotrypsin and papain (Fig. 4a). Of particular interest was the maintenance of catalytic function by WT and C95A (Fig. 4b,c). WT and C95A retained $\geq 85\%$ of activity after proteolysis. C56A and C145A, which did not exhibit SOD activity, were susceptible to proteolytic cleavage as evidenced by cleaved bands of low molecular weight on SDS-PAGE (Fig. 4a).

Circular dichroic spectroscopy (CD) analysis reveals enhanced conformational stability in C95A. CD-spectra for WT and C95A had a broad minimum at 208 nm (Fig. 5a) suggesting high percentage of β -sheet content as observed in human and most other eukaryotic SODs. For C56A and C145A, shift of CD-signal towards 200 nm was observed eliciting enhanced randomness in the structures. CD-spectra revealed highest conformational stability of C95A towards autoclaving. After autoclaving, C95A retained maximum

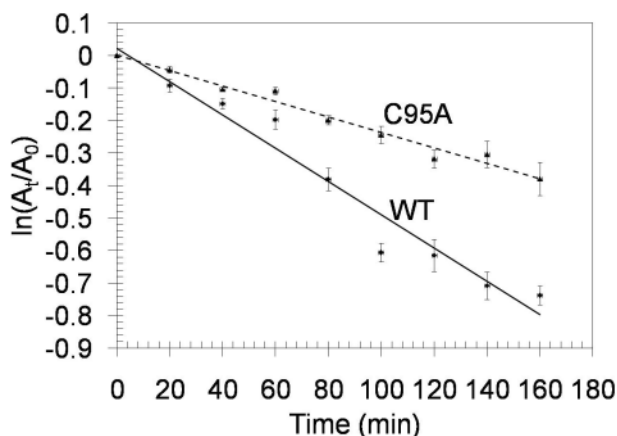


Figure 3 | Thermal inactivation kinetics of SOD. 1.0-ml solution of 0.2 mg/ml of each enzyme in 50 mM potassium phosphate buffer, pH 7.8, was incubated at 80°C for 160 min. Samples (100 μl) were removed after every 20 min and stored on ice. After 160 min, all samples were assayed for SOD activity under standard assay conditions using NBT-based assay. The data were fit as zero, first, and second order reactions¹⁸, wherein the first-order reaction gave the most linear relationship and shown in this Fig. 3. SOD activity was not detected for C56A and C145A, and hence corresponding activity curves are not shown. Solid and dashed lines represent WT and C95A, respectively. Values were mean \pm SE of three separate replicates. WT, wild type; C95A, cysteine at position 95 substituted with alanine. The above figure was also used to calculate various kinetic parameters as shown in Supplementary Table S1. The rate constant k_d (min^{-1}) and $t_{1/2}$ for first-order thermal inactivation were determined^{51,52} from “equation (1)” and “equation (2)”, respectively (equations described in “Methods” section). A_t , residual activity that remains after heating the enzyme for time t ; A_0 , initial enzyme activity before heating.

β -sheet content followed by WT (Supplementary Table S2). C56A and C145A had very low CD-signal after autoclaving and were the most labile structures (Fig. 5a and Supplementary Table S2).

Thermal-stability of un-autoclaved and autoclaved WT and mutants was further studied by recording CD-spectra at different temperatures upto 100°C (Fig. 5b). WT and C95A retained the secondary structure upto 60°C and a loss in their structure was recorded at higher temperatures. C56A and C145A exhibited randomness in structure at temperatures above 50°C .

Cysteine replacements affect the three dimensional structure related parameters of SOD: an *in silico* modeling analysis. Based on the three-dimensional structure of WT, obtained from X-ray crystallography with 2.1 \AA resolution⁸, models of WT, C56A, C95A, C145A were constructed. The deviations between these models were generally small for the backbone atoms (rmsd from 0.2 to 0.6 \AA). The constructed models also showed high verification scores when estimated using “Verify 3D Profile” tool of the DS. Differences were obtained for these three mutants for DOPE score, PDF total energy, and total molecular volume (Supplementary Table S3). The regions of deviations were visible after superimposing the generated models using WT (2q2l, subunit a). For C95A, the DOPE score and PDF total energy was found to be lowest amongst the four enzymes evaluated suggesting a more stable structure. Also, these mutants were analyzed using *Build Mutant* tool of the DS. The energy calculations revealed that C56A and C145A showed increase in the PDF total energy (33%) with respect to the WT, whereas C95A resulted in slight decrease (1%) in the PDF total energy.

Discussion

Role of cysteine in modulating kinetic properties of Cu,Zn SOD is still an enigma^{13,18–20,23,24}. Enormous work has been carried out in animal system, but there are no reports on the role of cysteine in any of the Cu,Zn SODs derived from plants. Since amino acid sequences of Cu,Zn SODs in plant and animals vary significantly hence any conclusions drawn for SODs derived from animals may not be valid for those derived from plants. Cu,Zn SOD from *P. atrosanguinea* provides a unique opportunity to understand the role of free Cys-95 since the native enzyme retains more than 80% of its activity upon autoclaving and functions at temperature ranging between sub-zero temperatures to more than 50°C with maximum activity at $0\text{--}4^\circ\text{C}$ ^{5,8}. WT has three cysteines, out of which Cys-56 and Cys-145 are involved in disulphide linkage, whereas Cys-95 remains free.

The analysis on relative difference in solvent accessibility criterion suggested free Cys-95 to be present on the dimer interface (Supplementary Fig. S2). The presence of Cys-95 on dimeric interface of WT enzyme subunits is likely to play an important role in subunit association. Contact network based observations, based on structurally critical long-range contacts, suggested a possible role of Cys-95 in oligomerization of WT enzyme (Supplementary Fig. S3). Possibility also exists that Cys-95 would interact with another Cys-95 through disulphide linkage to form oligomer. Interestingly, Cys-95 adopts a double conformation in subunit B⁸. Increased number of conformation possibilities decreases the protein stability by increasing the entropy of the protein in unfolded state²⁹. Thus restricting conformational possibilities of the unfolded state is important in lowering its entropy and prevent unfolding.

The *in silico* based propositions on the role of Cys-95 on oligomerization were evaluated by replacing free Cys-95 with Ala. Alanine was a choice in this replacement, since the amino acid eliminates side chain beyond the β carbon. Also, alanine neither imposes extreme electrostatic/steric effects, nor alters the main-chain conformation³⁰. This replacement increased monomer to dimer ratio to 33 fold in C95A as compared to that in WT (Fig. 1a,b). Interestingly, the specific activity of C95A was higher as compared to the WT (Fig. 2a),

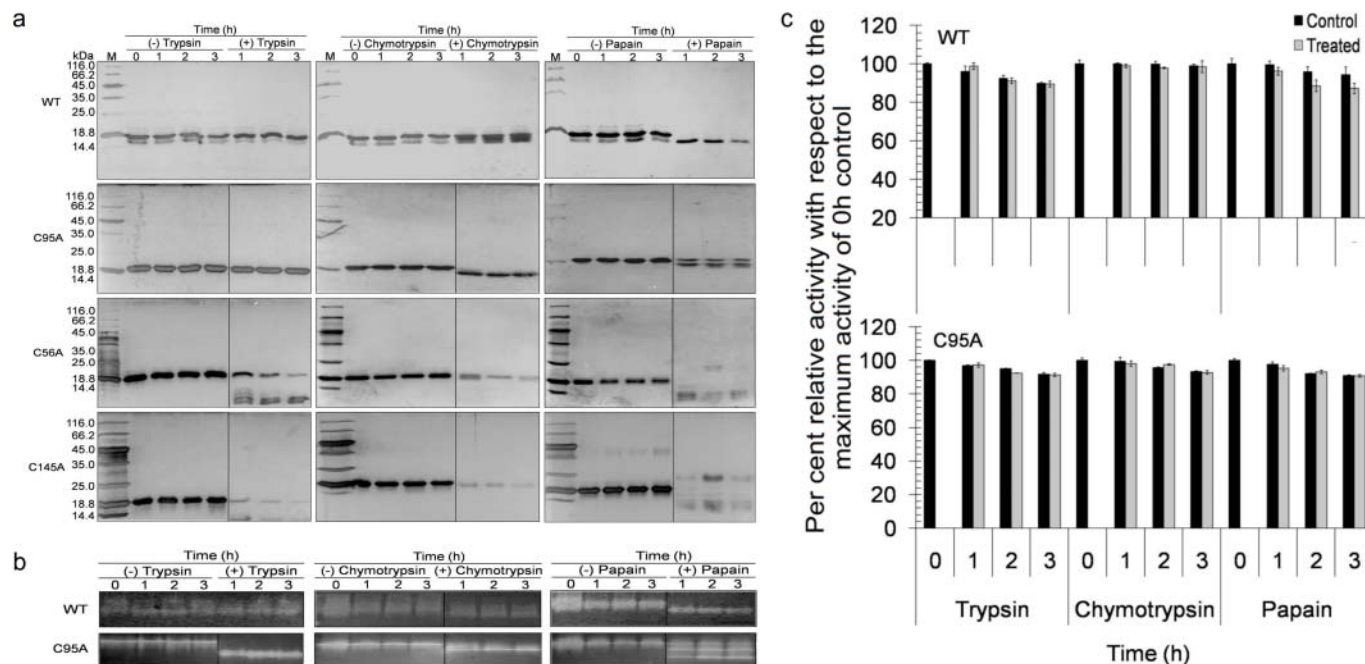


Figure 4 | Effect of incubation of SOD with proteolytic enzymes. SOD was incubated in the absence (-) and presence (+) of 1/20 w/w of trypsin, chymotrypsin or papain in 50 mM potassium phosphate buffer, pH 7.8, and 37°C for 1, 2, and 3 h and run on a SDS-PAGE (a). M, molecular weight marker procured from Fermentas, USA; the protein markers were β -galactosidase (11 6000 Da), bovine serum albumin (66 200 Da), Ovalbumin, 45 000 Da), lactate dehydrogenase (35 000 Da), REase Bsp981 (21 000), β -lactoglobulin (18 400) and lysozyme (14 400 Da)]. Full-length gels are shown in Supplementary Fig. S9a. Activity staining of protease treated SODs is shown in panel “b”. Protease treated SODs were run on native rather than SDS containing poly-acrylamide gel. Therefore, the migration pattern of SODs shows some variation between the panels (a) and (b). SOD activity was not detected for C56A and C145A, and hence corresponding SOD activity stained gels are not shown. Full-length gels are shown in Supplementary Fig. S9b. Panel (c) depicts the effect of proteolytic enzymes on SOD activity; values are mean \pm SE of three separate replicates. WT, wild type; C56A, cysteine at position 56 substituted with alanine; C95A, cysteine at position 95 substituted with alanine; C145A, cysteine at position 145 substituted with alanine.

suggesting that higher monomerization favored increased catalytic activity. Monomer as well dimer form of the Cu,Zn SOD is known to retain the catalytic activity^{11,31}. Depending upon the species under consideration the catalytic activity of the two forms could vary. For example, dimer exhibited comparatively higher activity in *Ipomoea batatas*³¹, and *Carica papaya*¹¹. Higher activity of dimer form was possibly due to improved enzyme conformation and stability of the enzyme¹¹. Monomerization led to an abrupt decrease in the catalytic activity of the enzyme either by alterations in the tertiary structure due to extensive solvation and/or distortion of the newly exposed dimer interface in Cu,Zn SOD from human^{13,32,33}. On the contrary, monomeric Cu,Zn SOD of *E. coli* retained the full catalytic activity, which suggested that dimeric form is not a requirement for the efficient catalytic activity by Cu,Zn SOD¹³. Substitution of a charged amino acid in place of a hydrophobic amino acid has been found to be responsible for monomerization³⁴. However, in C95A substitution of a uncharged polar amino acid with a hydrophobic amino acid (Ala) led to higher monomerization (Fig. 1a,b). Results were in consonance with the computational data that suggested the role of Cys-95 in interfacing with other amino acids to stabilize dimer of WT (Supplementary Fig. S3). The present data suggested the importance of higher monomer to dimer ratio for enhanced thermal tolerance as evident from the reduced (about half) k_d and increased $t_{1/2}$ (about twofold) values for C95A as compared to WT (Supplementary Table S1).

Lesser loss in activity after autoclaving and lower thermal inactivation in C95A as compared to WT suggested reduced irreversible denaturation in the former. The results were supported by CD data which showed a loss of 20% of β -sheet content upon autoclaving WT as compared to the un-autoclaved control. However, C95A exhibited an increase of 2.5% of β -sheet content upon autoclaving as compared

to the un-autoclaved control (Fig. 5a and Supplementary Table S2). These results are suggestive of retention of secondary structure of the autoclaved C95A as compared to the autoclaved WT.

Lower values of PDF physical energy and the DOPE score (Supplementary Table S3) also indicated C95A structure to be the least restrained. Since free cysteine might be the preferred site for oxidation of SOD molecules, it could impede the enzyme activity. It has been shown that human Cu,Zn SOD undergoes irreversible aggregation upon exposure to temperatures higher than their respective melting temperatures, which is attributed to the presence of free cysteine residues. Formation of improper disulfide-bonds, concomitant with cysteine oxidation has been attributed to heat-denatured aggregation³⁴. Mutation of free Cys-95 to Ala might eliminate any such possibility, and would render the protein more stable.

It was also observed that cysteine residues of intra-disulfide bond (Cys-56 and Cys-145) are important for functioning of WT, since mutation of these residues resulted in the loss of enzymatic activity. The results were strengthened by CD analysis where structural loss was observed for these mutants (Fig. 5a,b). The loss may be attributed to permanent unfolding which is usually combined with the formation of aggregates due to the exposed hydrophobic core³⁵. The aggregation of C56A and C145A observed on SDS-PAGE suggested inter or intra-molecular non-native disulfide linkages in the proteins. The loss in structure at higher temperatures could be assigned to the increased entropy with increased number of conformational possibilities, which is usually high in the unfolded state and low in the folded state. It has been proposed that cysteine disulfide bridges can decrease the entropy of the unfolded state of a protein and as such acts as a stabilizing factor³⁶. Disulfide bond links loop IV and β -strand 8h of WT and this linkage of the secondary-structure elements contribute to the stabilization of the SOD fold⁸. The active site is

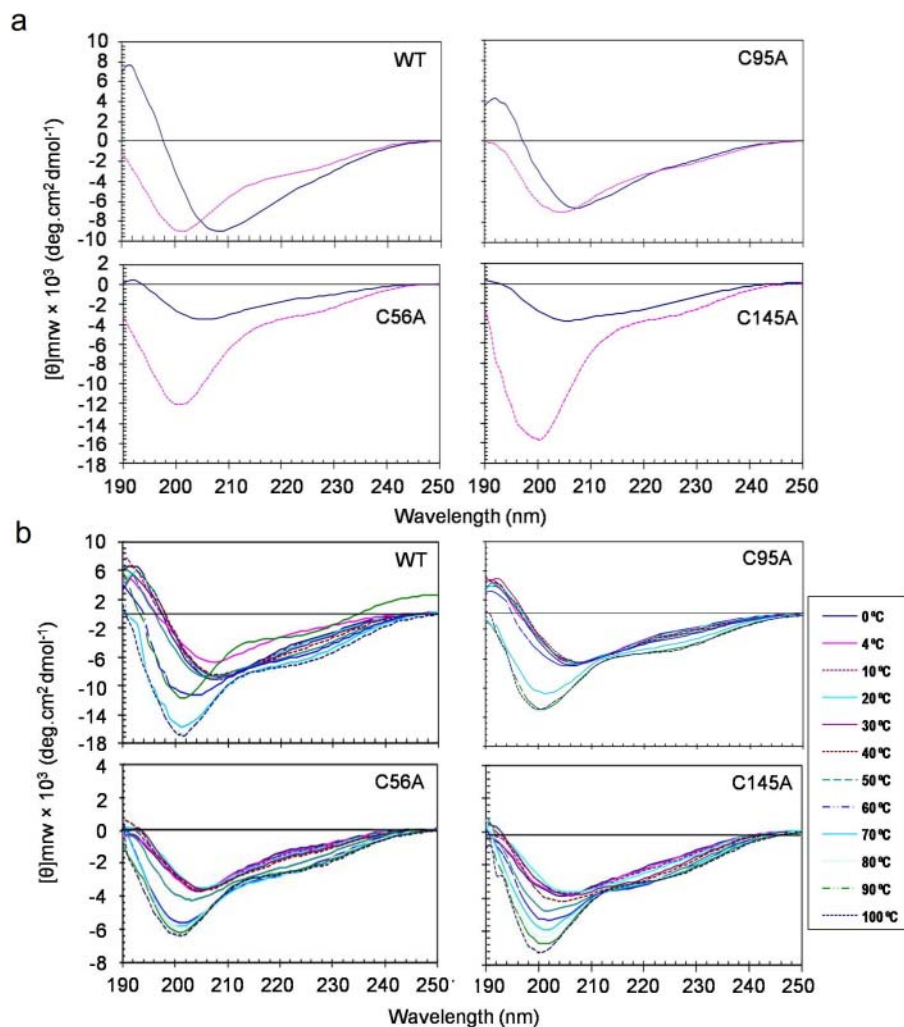


Figure 5 | Secondary structure analysis by CD-spectroscopy. Overlay of far-UV CD spectra of un-autoclaved and autoclaved enzymes (a). CD spectra were determined for each protein at a concentration of 0.2 mg/ml in 50 mM potassium phosphate buffer (pH 7.8) using a Jasco-815 spectropolarimeter (JASCO, Japan) maintained at 4°C. Far-UV (190–260 nm) CD spectra of protein was recorded in a quartz cuvette of 0.1 cm path length at a scan speed of 50 nm/min, with a 1 nm bandwidth, 1 nm data pitch and a 1 s response time. Solid (blue) and dashed (pink) lines represent un-autoclaved and autoclaved enzymes, respectively. Far-UV CD spectra of WT and mutant enzymes as a function of temperature is shown in panel “b”. CD spectra (190–260 nm) were recorded over a temperature range of 0–100°C in 50 mM potassium phosphate buffer (pH 7.8) in a quartz cuvette of 0.1 cm path length at a scan speed of 50 nm/min, with a 1 nm bandwidth, 1 nm data pitch and a 1 s response time. Spectra were analyzed every 10°C by incubating the protein (0.2 mg/ml) at defined temperature for 5 min for a temperature range of 0–100°C. WT, wild type; C56A, cysteine at position 56 substituted with alanine; C95A, cysteine at position 95 substituted with alanine; C145A, cysteine at position 145 substituted with alanine.

present at bottom of channel formed by two loops (IV and VII) which extends from β -barrel. Mutating cysteine residue in loop IV might destabilize WT and thereby decreased activity was recorded by affecting the active site. Graph-theoretical modelling studies revealed Cys-56 and Cys-145 to be critical for structural stability which was supported by our experimental work.

Resistance to proteolysis is a selection tool to assess protein stability^{37,38}. Also, proteolysis is used to probe energy states in proteins. Proteins are protected against proteolysis in their folded conformation, unless these have unstructured regions. In order to be digested, the substrates must access a high-energy state where cleavage sites are exposed to the solvent³⁹. Also proteolysis depends upon the accessible surface area. WT and C95A were found to be the least susceptible to cleavage by proteolytic enzymes trypsin and chymotrypsin at normal temperature. Papain partially digested both the enzymes (Fig. 4a), still the activity was retained upto 85 to 90% of the full activity (Fig. 4b,c). Results strengthened the hypothesis of a general correlation between the thermo-stability of proteins and their resistance to proteolysis³⁷.

Resistance of WT and C95A to proteolytic cleavage suggested that the protein has limited access to partially and globally unfolded conformations under native conditions⁴⁰. Proteolytic resistance might have been imparted due to minimized occurrence of accessible conformations susceptible to proteolytic attack. C56A and C145A were highly susceptible to proteolytic cleavage (Fig. 4a), possibly due to loss of structure of these mutants as evidenced from CD data (Fig. 5a,b) leading to increased access of the protein by trypsin, chymotrypsin and papain.

To conclude, the present study suggested the importance of increased monomer to dimer ratio to enhance thermostability of Cu,Zn SOD, wherein mutation of a free cysteine (Cys-95) played a central role. Data was supported by *in silico* as well as other biochemical parameters. The engineered SOD can be used for developing transgenic plants tolerant to abiotic stresses^{41,42}, particularly for high temperature and drought stress, where the temperature can rise to as high as 50–60°C⁴³. Herein, ROS mediated damages are inevitable. C95A reported in the present work, which



is tolerant as well as functional to higher temperature, would be a boon for such application.

Methods

Site directed mutagenesis. Coding sequence of WT (456 bp; GenBank Acc No., EU532614) was amplified and cloned in pQE-30 U/A expression vector^{8,44}. Polymerase chain reaction (PCR) was carried out to create mutation in SOD gene by using mutagenic primers (Supplementary Table S4) as described previously⁴⁵. In brief, PCR mix (25 μ l) contained 2.5 μ l of 10x long-amplicon (LA)-Taq polymerase buffer, 100 nM each of dATP, dTTP, dGTP, and dCTP; 100 ng of each forward and reverse primers; 25 ng plasmid pQE30-UA carrying SOD gene; 0.5 μ l (1.25 U) LA-Taq (Takara, Clontech, USA) and water to a final volume of 25 μ l. PCR product was digested with *Dpn*I and the resulting single stranded mutated DNA was transformed into *E. coli* XL1-Blue supercompetent cells (Stratagene, USA). Colonies were screened on LB ampicillin plates, plasmids were isolated using GenElute Plasmid Miniprep Kit (Sigma, USA) and sequencing was performed on an automated DNA sequencer (ABI Prism 3130xl, Applied Biosystems, USA) to confirm the incorporation of desired mutations. The mutated plasmids were transformed into *E. coli* M15 cells. Recombinant proteins were expressed and purified under native conditions by affinity based chromatography using Ni-NTA⁴⁴. Since, SOD is a homodimeric enzyme both subunits had the desired mutations.

SOD assay and protein estimation. Enzyme assay was performed as described previously^{46,47} except that the reaction was carried out using 1 μ g of the purified protein per assay in a 96 well plate maintained at 4°C (optimal temperature of the enzyme⁴⁴) in a final volume of 200 μ l. The absorbance was recorded at 560 nm using a microtitre plate reader (Synergy HT, with Gen5 controlling software, Biotek, USA). A control reaction was always carried out wherein 50 mM potassium phosphate buffer was added to the reaction mixture in lieu of the enzyme. Activity of SOD was expressed as units per mg protein. One unit of the enzyme activity was defined as the amount of enzyme required to inhibit nitro blue tetrazolium (NBT) reduction by 50%. Protein concentration was determined by Bradford method⁴⁸ using bovine serum albumin as a standard reference.

Assessing oligomerization status of the purified SODs. Oligomerization status was analyzed by electrophoresis under reducing and non-reducing conditions wherein equal quantities (1 μ g) of the proteins were run on 15% sodium dodecyl sulfate-polyacrylamide (SDS-PAGE)⁴⁹ gel in the presence and absence of 2-mercaptoethanol (2-ME)⁵⁰. Protein along with the sample loading buffer was boiled before loading onto SDS-PAGE. In a separate gel, the boiling step was omitted⁵⁰ and the protein separated on SDS-PAGE was stained for SOD activity⁴⁷.

Separation of monomer and dimer by size exclusion chromatography (SEC). Purified protein was filtered through 0.22 μ m filter and subjected to SEC using a SuperdexTM 75 10/300 GL (10 \times 300–310 mm) (GE Healthcare, UK) connected to an Äkta PrimeTM plus (GE Healthcare, UK) system. The column was equilibrated with 50 mM potassium phosphate buffer, pH 7.8, containing 40 mM KCl. Protein was applied in a volume of 500 μ l. The column was operated at 20°C at a flow rate of 0.5 ml min⁻¹. PrimeViewTM software was used for protein monitoring and 1.0 ml fractions were collected using an automated fraction collector. After SEC, fractions corresponding to monomeric and dimeric position were evaluated for protein estimation as described in earlier section.

Effect of mutations on enzyme activity. Enzyme was autoclaved (121°C, 1.1 kg/cm², 20 min) and the activity of un-autoclaved and the autoclaved enzyme was determined as described in earlier section. Further, 300 ng of each un-autoclaved and autoclaved enzyme was run on a native PAGE using 10% separating and 4% stacking gel¹⁹. After electrophoresis, gel was stained for activity¹⁷.

Enzyme assay was performed at temperatures ranging between (–) 10 to (+) 80°C. For assaying at sub-zero temperatures, 50% glycerol was added in the reaction mixture to avoid freezing and the assay was carried out by maintaining the temperature in a 96 well plate inside a deep freezer. SOD assay at temperatures ranging between (+) 10 to (+) 80°C was performed in 0.5 ml tubes maintained at desired assay temperatures on a thermo-mixer (Eppendorf, Germany). Separate blank and control reactions were performed for all assay temperatures.

Thermal inactivation assay. Thermal inactivation assay was performed¹⁸ with minor modifications. Purified enzyme was diluted to prepare 1-ml solution containing 0.2 mg/ml protein in 50 mM potassium phosphate buffer, pH 7.8. For each 1 ml of the enzyme solution, a 100- μ l of the initial sample was removed and stored on ice (0 min). Thereafter, the enzyme solution was heated in a water bath at 80°C. Every 20 min, a 100 μ l aliquot was removed till 160 min, stored on ice and assayed for residual SOD activity. The thermal inactivation data for WT and C95A was plotted for zero (residual activity versus time), first (natural logarithm of the residual activity versus time) and second order (reciprocal activity versus time)¹⁸. The rate constant k_4 (min⁻¹) for first-order thermal inactivation was determined⁵¹ from the slope of the inactivation time course according to the “equation (1)”, $\ln(A_t/A_0) = -k_4 t$. Where A_t is the residual activity that remains after heating the enzyme for time t , and A_0 is the initial enzyme activity before heating. The half-time of thermal inactivation ($t_{1/2}$) was determined⁵² following the “equation (2)”, $t_{1/2} = \ln(2)/k_4$.

Limited proteolysis of enzymes. Enzymes were incubated with 1/20 w/w of trypsin, chymotrypsin or papain in 50 mM potassium phosphate buffer, pH 7.8, and 37°C for defined time intervals. For chymotrypsin digestion, CaCl₂ was added to a final concentration of 20 mM in the buffer. For digestion with papain, cysteine was added to a final concentration of 5 mM in the buffer. Control samples were incubated under identical conditions but without the proteolytic enzyme. Aliquots were removed at defined time intervals and analyzed on 15% SDS-PAGE for protein integrity. Samples were also evaluated for activity on 10% native-PAGE.

Circular dichroic spectroscopy and secondary structure estimation. Circular dichroic (CD) spectra were recorded on a JASCO J-815 spectropolarimeter equipped with a peltier thermostatic cell holder (model PTC- 423S/15; JASCO, Japan). Spectropolarimeter was pre-calibrated with 0.6% (w/v) aqueous ammonium (+)-camphor-10-sulphonate. The enzymes were dialyzed three times against 50 mM potassium phosphate buffer (pH 7.8). Far-UV (190–260 nm) CD spectra of enzyme (0.2 mg/ml) was recorded at 4°C and 25°C in a quartz cuvette of 0.1 cm path length at a scan speed of 50 nm/min, with a 1 nm bandwidth, 1 nm data pitch and a 1 s response time. For thermal scans, the enzyme samples (0.2 mg/ml) were heated from 0 to 100°C with a heating rate of 5°C/min controlled by a JASCO programmable peltier element. Far-UV CD spectrum was recorded every 10°C and the dichroic activity was monitored continuously. The results were expressed as mean residue ellipticity (θ) by calculating mean residue weight per amino acid residue. Each spectrum was the mean of three accumulated scans. All values were corrected for solvent contributions. Molar ellipticity per residue (θ), expressed in deg.cm².dmol⁻¹, was calculated using the “equation (3)”, $\theta_{MRE} = MRW \Theta_{obs} / 10cl$, where Θ is the ellipticity observed (mdeg), MRW is the mean residue weight per amino acid residue, c is protein concentration (mg/ml), and l is path length of the cuvette (cm). To estimate the proportions of secondary structures (α -helix, β -sheet, turns, random or unordered forms), the reference CD spectra obtained by Yang were used⁵³. The software supplied by JASCO, Japan was used for analyzing the data.

Molecular model-building. Models of three-dimensional structures of WT, C56A, C95A, and C145A were constructed using homology modeling approach. Structural based alignment was performed using Discovery Studio (DS) software package (M/S Accelrys, version 2.1, USA). X-ray crystallographic structure of WT (Protein Data Bank accession no. 2q2l) was used as a template structure. Root mean square deviation (RMSD), probability density function (PDF), total energy, molecular volume, and discrete optimized protein energy (DOPE) scores were calculated using the DS software. Model accuracy was determined by estimating the superimposition using “Verify 3D Profile” program of the DS.

- Getzoff, E. D. *et al.* Faster superoxide dismutase mutants designed by enhancing electrostatic guidance. *Nature* **358**, 347–351 (1992).
- Desideri, A. *et al.* Evolutionary conservativeness of electric field in the Cu,Zn superoxide dismutase active site. *J. Mol. Biol.* **223**, 337–342 (1992).
- Liochev, S. I. & Fridovich, I. Copper- and zinc-containing superoxide dismutase can act as a superoxide reductase and a superoxide oxidase. *J. Biol. Chem.* **275**, 38482–38485 (2000).
- Halliwell, B. & Gutteridge, J. M. Role of free radicals and catalytic metal ions in human disease: an overview. *Methods Enzymol.* **186**, 1–85 (1990).
- Kumar, S., Sahoo, R. & Ahuja, P. S. Isozyme of autoclavable superoxide dismutase (SOD), a process for the identification and extraction of the SOD in cosmetic, food and pharmaceutical compositions. *US Patent No. 6,485,950 B1* (2002).
- Bafana, A., Dutt, S., Kumar, S. & Ahuja, P. S. Superoxide dismutase: an industrial perspective. *Crit. Rev. Biotechnol.* **31**, 65–76 (2011).
- Bafana, A., Dutt, S., Kumar, A., Kumar, S. & Ahuja, P. S. The basic and applied aspects of superoxide dismutase. *J. Mol. Catal. B: Enzym.* **68**, 129–138 (2011).
- Yogavel, M. *et al.* Structure of a superoxide dismutase and implications for copper-ion chelation. *Acta Crystallogr. D: Biol. Crystallogr.* **D64**, 892–901 (2008).
- Parge, H. E., Getzoff, E. D., Scandella, C. S., Hallewell, R. A. & Tainer, J. A. Crystallographic characterization of recombinant human CuZn superoxide dismutase. *J. Biol. Chem.* **261**, 16215–16218 (1986).
- Ken, C. F., Weng, D. F., Duan, K. J. & Lin, C. T. Characterization of copper/zinc-superoxide dismutase from *Pagrus major* cDNA and enzyme stability. *J. Agric. Food Chem.* **50**, 784–789 (2002).
- Lin, C. T., Kuo, T. J., Shaw, J. F. & Kao, M. C. Characterization of the dimer-monomer equilibrium of the papaya copper/zinc superoxide dismutase and its equilibrium shift by a single amino acid mutation. *J. Agric. Food Chem.* **47**, 2944–2949 (1999).
- Lin, M. W., Lin, M. T. & Lin, C. T. Copper/zinc-superoxide dismutase from lemon cDNA and enzyme stability. *J. Agric. Food Chem.* **50**, 7264–7270 (2002).
- Battistoni, A., Folcarelli, S., Gabbianelli, R., Capo, C. & Rotilio, G. The Cu,Zn superoxide dismutase from *Escherichia coli* retains monomeric structure at high protein concentration. Evidence for altered subunit interaction in all the bacteriocupreins. *Biochem. J.* **320**, 713–716 (1996).
- Malinowski, D. P. & Fridovich, I. Subunit association and side-chain reactivities of bovine erythrocyte superoxide dismutase in denaturing solvents. *Biochemistry* **18**, 5055–5060 (1979).
- Forman, H. S. & Fridovich, I. On the Stability of Bovine Superoxide Dismutase: The effects of metals. *J. Biol. Chem.* **248**, 2645–2649 (1973).



16. Vetriani, C. *et al.* Protein thermostability above 100°C: A key role for ionic interactions. *Proc. Natl. Acad. Sci. USA* **95**, 12300–12305 (1998).
17. Kumar, S. & Nussinov, R. How do thermophilic proteins deal with heat? *Cell. Mol. Life Sci.* **58**, 1216–1233 (2001).
18. McRee, D. E. *et al.* Changes in crystallographic structure and thermostability of a Cu,Zn superoxide dismutase mutant resulting from the removal of buried free cysteine. *J. Biol. Chem.* **265**, 14234–14241 (1990).
19. Ken, C. F., Lin, C. T., Wen, Y. D. & Wu, J. L. Replacement of buried cysteine from zebrafish Cu/Zn superoxide dismutase and enhancement of its stability via site-directed mutagenesis. *Mar. Biotechnol.* **9**, 335–342 (2007).
20. Di Patti, M. C. B. *et al.* A free cysteine residue at the dimer interface decreases conformational stability of *Xenopus laevis* copper,zinc superoxide dismutase. *Arch. Biochem. Biophys.* **377**, 284–289 (2000).
21. Deng, H. X. *et al.* Amyotrophic lateral sclerosis and structural defects in Cu,Zn superoxide dismutase. *Science* **261**, 1047–1051 (1993).
22. Hörnberg, A., Logan, D. T., Marklund, S. L. & Oliveberg, M. The coupling between disulphide status, metallation and dimer interface strength in Cu/Zn superoxide dismutase. *J. Mol. Biol.* **365**, 333–342 (2007).
23. Amaki, Y., Nakano, H. & Yamane, T. Role of cysteine residues in esterase from *Bacillus stearothermophilus* and increasing its thermostability by the replacement of cysteines. *Appl. Microbiol. Biotechnol.* **40**, 664–668 (1994).
24. Arnold, L. D. & Lepock, J. R. Reversibility of the thermal denaturation of yeast superoxide dismutase. *FEBS Lett.* **146**, 302–306 (1982).
25. Battistoni, A. *et al.* Role of the Dimeric Structure in Cu,Zn Superoxide Dismutase: pH-dependent, reversible denaturation of the monomeric enzyme from *Escherichia coli*. *J. Biol. Chem.* **273**, 5655–5661 (1998).
26. Bourne, Y. *et al.* Novel dimeric interface and electrostatic recognition in bacterial Cu,Zn superoxide dismutase. *Proc. Natl. Acad. Sci. USA* **93**, 12774–12779 (1996).
27. Porollo, A., Adamczak, R. & Meller, J. POLYVIEW: a flexible visualization tool for structural and functional annotations of proteins. *Bioinformatics* **20**, 2460–2462 (2004).
28. Ratha, A., Glibowicka, M., Nadeau, V. G., Chen, G. & Deber, C. M. Detergent binding explains anomalous SDS-PAGE migration of membrane proteins. *Proc. Natl. Acad. Sci. USA* **106**, 1760–1765 (2009).
29. Matthews, B. W., Nicholson, H. & Matthews, B. W., Nicholson, H. & Becktel, W. J. Enhanced protein thermostability from site-directed mutations that decrease the entropy of unfolding. *Proc. Natl. Acad. Sci. USA* **84**, 6663–6667 (1987).
30. Lefèvre, F., Rémy, M. H. & Masson, J. M. Alanine-stretch scanning mutagenesis: a simple and efficient method to probe protein structure and function. *Nuc. Acids Res.* **25**, 447–448 (1997).
31. Lin, C. T., Lin, M. T., Chen, Y. T. & Shaw, J. F. Subunit interaction enhances enzyme activity and stability of sweet potato cytosolic Cu/Zn-superoxide dismutase purified by a His-tagged recombinant protein method. *Plant Mol. Biol.* **28**, 303–311 (1995).
32. Banci, L. *et al.* Solution structure of reduced monomeric Q133M2 copper, zinc superoxide dismutase (SOD). Why is SOD a dimeric enzyme? *Biochemistry* **37**, 11780–11791 (1998).
33. Bertini, I., Piccioli, M., Viezzoli, M. S., Chiu, C. Y. & Mullenbach, G. T. A spectroscopic characterization of a monomeric analog of copper, zinc superoxide dismutase. *Eur. Biophys. J.* **23**, 167–176 (1994).
34. Khare, S. D., Ding, F. & Dokholyan, N. V. Folding of Cu, Zn superoxide dismutase and familial amyotrophic lateral Sclerosis. *J. Mol. Biol.* **334**, 515–525 (2003).
35. Chiti, F. *et al.* Studies of the aggregation of mutant proteins in vitro provide insights into the genetics of amyloid diseases. *Proc. Natl. Acad. Sci. USA* **99**, 16419–16426 (2002).
36. Pace, N. C., Grimsley, G. R., Thomson, J. A. & Barnett, B. J. Conformational stability and activity of ribonuclease T1 with zero, one, and two intact disulfide bonds. *J. Biol. Chem.* **263**, 11820–11825 (1988).
37. Daniel, R. M., Cowan, D. A., Morgan, H. W. & Curran, M. P. A correlation between protein thermostability and resistance to proteolysis. *Biochem. J.* **207**, 641–644 (1982).
38. Parcell, D. A. & Sauer, R. T. The structural stability of a protein is an important determinant of its proteolytic susceptibility in *Escherichia coli*. *J. Biol. Chem.* **264**, 7590–7595 (1989).
39. Park, C. & Marqusee, S. Probing the High Energy States in Proteins by Proteolysis. *J. Mol. Biol.* **343**, P1467–1476 (2004).
40. Manning, M. & Colon, W. Structural basis of protein kinetic stability: resistance to sodium dodecyl sulfate suggests a central role for rigidity and a bias toward beta-sheet structure. *Biochemistry* **43**, 11248–11254 (2004).
41. Gupta, A. S., Heinen, J. L., Holaday, A. S., Burket, J. J. & Allen, R. D. Increased resistance to oxidative stress in transgenic plants that overexpress chloroplastic Cu/Zn superoxide dismutase. *Proc. Natl. Acad. Sci. USA* **90**, 1629–1633 (1993).
42. Foyer, C. H., Descourvières, P. & Kunert, K. J. Protection against oxygen radicals: an important defence mechanism studied in transgenic plants. *Plant Cell Environ* **17**, 507–523 (1994).
43. Iba, K. Acclimative response to temperature stress in higher plants: approaches of gene engineering for temperature tolerance. *Annu. Rev. Plant Biol.* **53**, 225–245 (2002).
44. Bhardwaj, P. K., Sahoo, R., Kumar, S. & Ahuja, P. S. Superoxide dismutase (SOD) gene and a method of identifying and cloning thereof. *US Patent 7,888,088 B2* (2011).
45. Sambrook, J. & Russel, D. W. *Molecular Cloning: A Laboratory Manual*, 3rd ed. (Cold Spring Harbor Laboratory Press, Cold Spring Harbor, NY, 2001).
46. Beauchamp, C. & Fridovich, I. Superoxide dismutase: improved assays and an assay applicable to acrylamide gels. *Anal. Biochem.* **44**, 276–287 (1971).
47. Vyas, D., Kumar, S. & Ahuja, P. S. Tea (*Camellia sinensis*) clones with shorter periods of winter dormancy exhibit lower accumulation of reactive oxygen species. *Tree Physiol.* **27**, 1253–1259 (2007).
48. Bradford, M. M. A rapid and sensitive method for the quantitation of microgram quantities of protein utilizing the principle of protein-dye binding. *Anal. Biochem.* **72**, 248–254 (1976).
49. Laemmli, U. K. Cleavage of structural proteins during the assembly of the head of bacteriophage T4. *Nature* **227**, 680–685 (1970).
50. Peterson, S. V. *et al.* The dual nature of human extracellular superoxide dismutase: One sequence and two structures. *Proc. Natl. Acad. Sci. USA* **100**, 13875–13880 (2003).
51. Lawton, J. M. & Doonan, S. Thermal inactivation and chaperonin-mediated renaturation of mitochondrial aspartate aminotransferase. *Biochem. J.* **334**, 219–224 (1998).
52. Johannes, T. W., Woodyer, R. D. & Zhao, H. Directed evolution of a thermostable phosphite dehydrogenase for NAD(P)H regeneration. *Appl. Environ. Microbiol.* **71**, 5728–5734 (2005).
53. Yang, J. T., Wu, C. S. & Martinez, H. M. Calculation of protein conformation from circular dichroism. *Methods Enzymol.* **130**, 208–269 (1986).

Acknowledgements

Authors thank Council of Scientific and Industrial Research (CSIR) for funding through mission mode project on “exploratory studies on climate change and adaptation of species complex” NWP020. AK gratefully acknowledges CSIR for senior research fellowship. Technical help provided by Digvijay Singh Naruka in sequencing is duly acknowledged. Manuscript represents IHBT communication number 2292. The work has been applied for patent vide number NF0050/2011 dated 11.4.2011, 1031del 2011 India.

Author contributions

AK conducted the actual bench work, collected, analyzed and interpreted the data, collected the literature and drafted the manuscript. SD performed N-terminal amino acid sequencing, *in silico* analysis using Discovery Studio and assisted in mass spectrometric analysis. GB carried out computational analysis. PSA supported the work. SK conceived the idea, designed and guided the research, interpreted the data, linked various components and wrote the manuscript. All the authors have read the manuscript and agree with the content.

Additional information

Supplementary information accompanies this paper at <http://www.nature.com/scientificreports>

Competing financial interests: Authors declare that they have no competing financial interests.

License: This work is licensed under a Creative Commons Attribution-NonCommercial-ShareAlike 3.0 Unported License. To view a copy of this license, visit <http://creativecommons.org/licenses/by-nc-sa/3.0/>

How to cite this article: Kumar, A., Dutt, S., Bagler, G., Ahuja, P. S. & Kumar, S. Engineering a thermo-stable superoxide dismutase functional at sub-zero to >50°C, which also tolerates autoclaving. *Sci. Rep.* **2**, 387; DOI:10.1038/srep00387 (2012).